

Structural and Dynamic Studies of Zinc, Gallium, and Cadmium Complexes of a Dicarboxylate Pendant-Armed Cross-Bridged Cyclen

Weijun Niu,^[a] Edward H. Wong,^{*,[a]} Gary R. Weisman,^{*,[a]} Yijie Peng,^[a] Carolyn J. Anderson,^[b] Lev N. Zakharov,^[c] James A. Golen,^{[c],†} and Arnold L. Rheingold^[c]

Keywords: Zinc / Gallium / Cadmium / Cyclen / Cross-bridged ligand / Pendant arms

Zn^{II}, Ga^{III}, and Cd^{II} complexes of a dicarboxylate pendant-armed derivative of an important new cross-bridged cyclen ligand were prepared and characterized spectrally. Crystal structures of the Zn^{II} and Ga^{III} complexes both feature pseudo-octahedral metal centers, fully enveloped by the ligand's *cis*-N₄O₂ donor set with the zinc coordination sphere less distorted. All Ga–N and Ga–O bonds are significantly shorter than the corresponding values in the zinc structure.

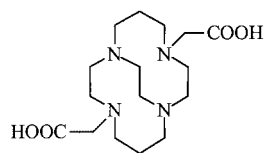
Solution NMR spectral studies revealed dynamic enantiomerization for the Zn^{II} complex with $\Delta G^\ddagger = 12.3(1)$ kcal/mol (24 °C). By contrast, the Ga^{III} complex gave only slow-exchange limit spectra up to the highest temperature measured [87(2) °C; $\Delta G^\ddagger > 21.1(2)$ kcal/mol].

(© Wiley-VCH Verlag GmbH & Co. KGaA, 69451 Weinheim, Germany, 2004)

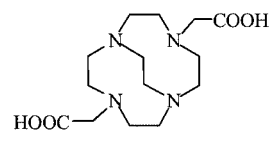
Introduction

The enhanced kinetic inertness imparted to metal complexes formed by cross-bridged cyclam and cyclen ligands has generated interest in the catalytic as well as radiopharmaceutical potentials of these ligands.^[1–4] This superior inertness towards decomplexation even under highly acidic or oxidizing conditions, which discourages common decomplexation pathways, is a consequence of our ligand design.^[5–7] While the importance of accessible, ancillary *cis*-coordination sites for catalytic or biomimetic applications has been noted^[8–10] for carriers of radiometals such as ⁶⁴Cu, ⁶⁷Ga, and ¹¹¹In, complete envelopment of such cations within the chelator is desirable to ensure even more inert complexes.^[11–13] *N*-Functionalization of the parent ligands with pendant arms containing additional donor sites is an effective way to attain this goal. We have already reported a dicarboxylate-armed cyclam ligand, CB-

H₂TE2A, and its copper(II) complex, Cu-CB-TE2A, as well as its cyclen analogue, Cu-CB-DO2A.^[2,7] Their *in vivo* behavior using ⁶⁴Cu labelling has also been investigated.^[1,2] Herein, we report the syntheses and spectral characterizations of the zinc(II), gallium(III), and cadmium(II) complexes of the dicarboxylate pendant-armed cross-bridged cyclen CB-H₂DO2A (ligand H₂ 1).^[14,15] Their diamagnetic nature makes solution NMR spectral studies possible. X-ray structures of both the Zn^{II} and Ga^{III} complexes were determined. These d¹⁰-cations are without ligand-field stabilization factors and offer the opportunity to compare charge and size effects on coordination preferences.



CB-H₂TE2A



CB-H₂DO2A

^[a] Department of Chemistry, University of New Hampshire, Durham, New Hampshire 03824, USA
Fax: (internat.) + 1-603-862-4278
E-mail: ehw@cisunix.unh.edu
gary.weisman@unh.edu

^[b] Mallinckrodt Institute of Radiology, Washington University School of Medicine, St. Louis, MO 63110, USA
Fax: (internat.) + 1-314-362-9940
E-mail: AndersonCJ@mir.wustl.edu

^[c] Department of Chemistry and Biochemistry, University of California, San Diego, La Jolla, California 92093, USA
E-mail: arnrhein@chem.ucsd.edu

^[†] On leave from the Department of Chemistry and Biochemistry, University of Massachusetts Dartmouth, North Dartmouth, Massachusetts 02747, USA

Results and Discussion

Synthesis

In the presence of a stoichiometric amount of aqueous NaOH, cross-bridged ligand H₂ 1 and hydrated Zn(ClO₄)₂ or Cd(ClO₄)₂ formed a cloudy solution in methanol after refluxing. Upon filtration to remove a small amount of white precipitate and ether diffusion into the supernatant,

in each case, pure crystals of the neutral complexes co-crystallized with sodium perchlorate, $[\text{Zn}\cdot\mathbf{1}](\text{NaClO}_4)_{1.5}$ and $[\text{Cd}\cdot\mathbf{1}](\text{NaClO}_4)$, were obtained as revealed by both IR spectral and analytical data. To synthesize the gallium complex, equivalent amounts of the ligand and $\text{Ga}(\text{NO}_3)_3$ with sodium acetate as the base were refluxed in methanol. The resulting white precipitate was redissolved in aqueous methanol and diffusion of a mixture of diethyl ether and methanol into this solution yielded clear crystals of the complex $[\text{Ga}\cdot\mathbf{1}]\text{NO}_3$.

Infrared Data

The solid-state IR spectra of all isolated complexes contained strong carboxylate stretches and those of the Zn^{II} and Cd^{II} complexes occur between 1595 and 1645 cm^{-1} . By contrast, the Ga^{III} complex has its carboxylate bands at significantly higher frequencies (1672 and 1692 cm^{-1}). In addition, strong stretching bands are also observed for the nitrate (1284–1363 cm^{-1}) or perchlorate (1091–1107 cm^{-1}) anion in the respective complex.

NMR Spectral Data

The ^1H NMR spectrum of $\text{Zn}\cdot\mathbf{1}$ in CD_3OD (or D_2O) is indicative of time-averaged C_{2v} symmetry. This is most clearly shown by the downfield singlet resonance of the pendant-arm methylene protons (see Figure 1, top).

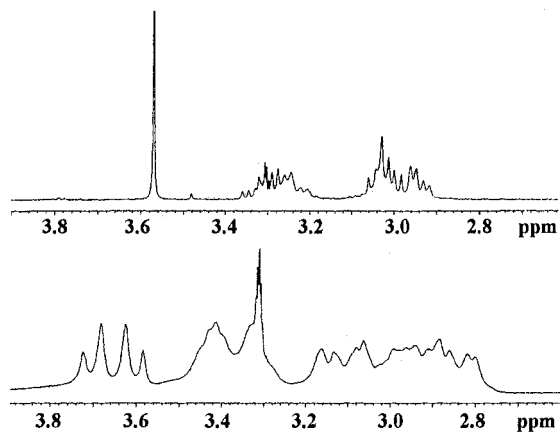


Figure 1. Variable-temperature 400 MHz ^1H NMR spectra of $\text{Zn}\cdot\text{CB-DO2A}$ in CD_3OD at 24 °C (top) and at -80 °C (bottom)

Likewise, the $^{13}\text{C}\{^1\text{H}\}$ NMR spectrum exhibits only four methylene ^{13}C resonances (two broad), in keeping with C_{2v} symmetry (see Figure 2, top). These data are in contrast to the solid-state X-ray structure, which approximates C_2 symmetry (vide infra) and suggest onset of a dynamic solution enantiomerization (see Figure 3). This was confirmed by the low-temperature NMR spectra in CD_3OD at -80 °C. While this proton spectrum contains broad and poorly resolved resonances in the upfield region, the pendant-arm CH_2 signal is clearly resolved into the AB pattern of diastereotopic methylene protons expected for C_2 symmetry (see Figure 1, bottom). Similarly, two of the four methylene ^{13}C resonances are resolved into two separate signals each

at low temperature (see Figure 2, bottom). Complete lineshape analysis of the broadest carbon resonance at 24(2) °C (see Exp. Sect.), which is in intermediate fast exchange, allows us to calculate a free energy of activation of 12.3(1) kcal/mol for the enantiomerization. Either a dissociative process involving detachment of pendant arms or a non-dissociative pseudorotation mechanism is consistent with the observed dynamic behavior.

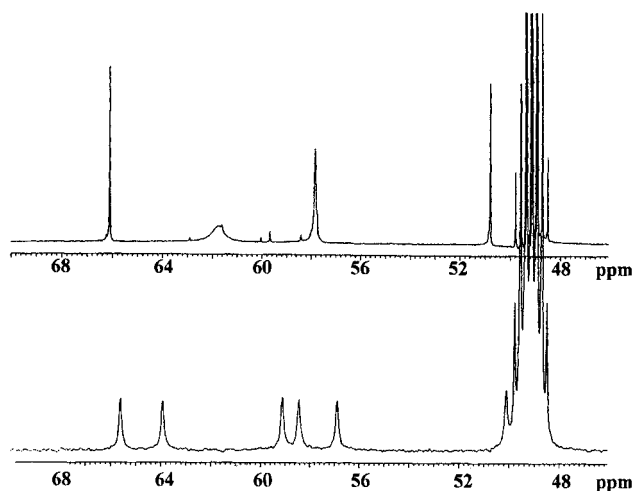


Figure 2. Variable-temperature 100 MHz $^{13}\text{C}\{^1\text{H}\}$ NMR spectra of $\text{Zn}\cdot\text{CB-DO2A}$ in CD_3OD at 24 °C (top) and at -80 °C (bottom)

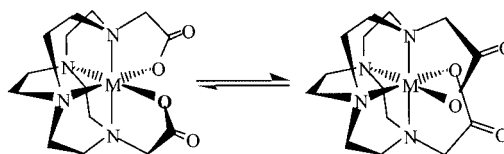


Figure 3. Enantiomerization of the zinc(II) complex of CB-DO2A

Both the proton and $^{13}\text{C}\{^1\text{H}\}$ NMR spectra of $[\text{Cd}\cdot\mathbf{1}]$ at room temperature in D_2O (see Exp. Sect.) are similar to the Zn^{II} complex data, again indicative of averaged C_{2v} solution symmetry on the NMR timescale. In addition, satellites due to $^{111,113}\text{Cd}$ coupling can also be observed in several of the ^1H as well as ^{13}C resonances. These attest to the integrity of the complex in solution since such couplings would be lost upon facile ligand exchange.

Unlike the zinc and cadmium complexes, at ambient temperature $[\text{Ga}\cdot\mathbf{1}]\text{NO}_3$ in D_2O gave proton and $^{13}\text{C}\{^1\text{H}\}$ NMR spectra consistent with a solution structure of C_2 symmetry (see Figure 4 and Exp. Sect.) in agreement with its X-ray structure (vide infra). The pendant-arm CH_2 protons exhibit an AB pattern with an additional W-long-range doublet coupling to the B portion of the subspectrum (apparent AB of ABX, although even this is an oversimplification since the X proton must be further coupled as well). Six signals having no dynamic broadening are observed in the methylene region of the $^{13}\text{C}\{^1\text{H}\}$ spectrum. Thus, enantiomerization is in the slow exchange limit on

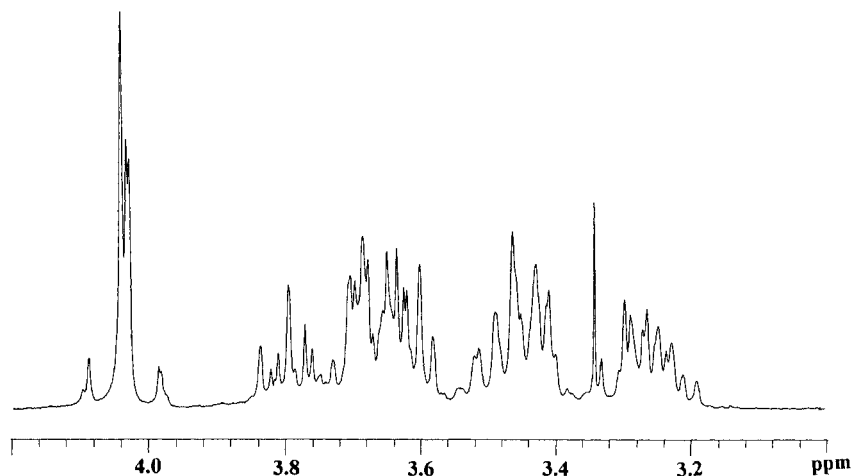


Figure 4. 360 MHz ^1H NMR spectrum of $[\text{Ga-CB-DO2A}]\text{NO}_3$ in D_2O

the ^1H and ^{13}C NMR timescales in solution at room temperature. High-temperature ^1H NMR spectra up to 87(2) $^\circ\text{C}$ show no dynamic broadening of the AB portion of the pendant-arm ABX multiplet. (Interestingly, the integration of this multiplet decreases over time, indicating significant H/D exchange.) Complete lineshape simulations of $\text{AB} \rightarrow \text{BA}$ dynamic exchange of the apparent ABX subspectrum of the pendant-arm CH_2 protons allow us to place a lower limit of 21.0(2) kcal/mol on the enantiomerization barrier at 87(2) $^\circ\text{C}$. This dramatic increase in going from $\text{Zn}\cdot\mathbf{1}$ to $[\text{Ga}\cdot\mathbf{1}]^+$ may be attributed to the higher cationic charge at the Ga^{III} center and stronger metal–ligand bonds, which may inhibit any dissociative process involving the coordinated carboxylate pendant arms. The X-ray solid-state structural comparison between $[\text{Zn}\cdot\mathbf{1}]$ and $[\text{Ga}\cdot\mathbf{1}]^+$ in the next section lends support to this premise. Since this gallium complex does not rapidly enantiomerize, we can further conjecture that pendant-arm dissociation rather than non-dissociative pseudorotation is most likely the relevant dynamic process.

X-ray Structural Data

The core structure of the zinc complex $[\text{Zn}\cdot\mathbf{1}]$ is shown in Figure 5. The Zn^{II} cation is fully enveloped within the *cis*- N_4O_2 donor set of the cross-bridged ligand in a near-octahedral geometry. The axial $\text{N}(2)\text{--Zn}(1)\text{--N}(4)$ angle of 178.32(6) [176.07(6)] $^\circ$ (structural data for a second independent molecule are given in brackets) is close to linearity, showing an unusually good fit for Zn^{II} within the cross-bridged cyclen cavity. Previous structural data of zinc complexes of the cross-bridged cyclen and its derivatives have shown the cation significantly distended from the ligand cavity with much more distorted axial N--Zn--N angles of between 148 and 159 $^\circ$.^[16–18] Another manifestation of these distortions can also be seen in their longer axial N--Zn bonds (2.17–2.26 Å) compared to the average of 2.12 Å found in $\text{Zn}\cdot\mathbf{1}$. The near-octahedral coordination geometry around $\text{Zn}(1)$ here can also be seen in the $\text{N}(1)\text{--Zn}(1)\text{--O}(3)$ angle of 172.30(6) [170.20(6)] $^\circ$ and the

$\text{N}(3)\text{--Zn}(1)\text{--O}(1)$ angle of 173.95(6) [174.18(6)] $^\circ$. Indeed, all Zn--N and Zn--O bond lengths are within a relatively narrow range of 2.067–2.177 Å. Selected bond lengths and angles are shown in Table 1. An X-ray structure of a DOTA complex of zinc(II) featuring a related *cis*- N_4O_2 ligand coordination mode has been reported.^[19] This has an axial N--Zn--N angle of 153.9 $^\circ$, an axial Zn--N distance of 2.232 Å, an equatorial Zn--N distance of 2.171 Å, and a shorter Zn--O distance of 2.037 Å. However, without the cross-bridging ethylene, the equatorial N--Zn--N angle is opened up to 107.8 $^\circ$ [compared to the 83.84(6) $^\circ$ for $\text{N}(1)\text{--Zn}(1)\text{--N}(3)$ here]. Also, in the reported structure the coordinated carboxylate pendant arms are on the equatorial macrocyclic nitrogen atoms rather than the axial ones and the DOTA structure is thus close to C_{2v} symmetry.

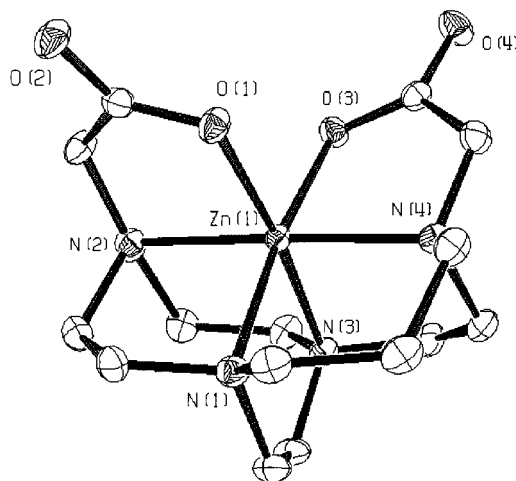


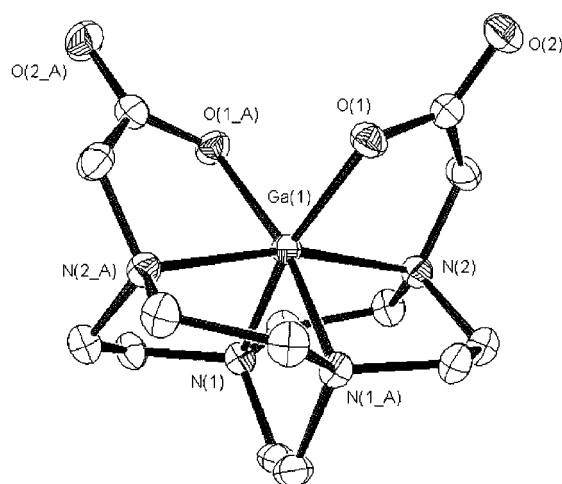
Figure 5. Molecular structure of $\text{Zn-CB-DO2A}\cdot\text{NaClO}_4$; hydrogen atoms and sodium perchlorate have been omitted for clarity

The X-ray structure of $[\text{Ga}\cdot\mathbf{1}]\text{NO}_3$ also reveals a fully enveloped Ga^{III} cation within the ligand's cleft (see Figure 6). The distortion from an idealized octahedral geometry is more pronounced here with an axial $\text{N}(2)\text{--Ga}(1)\text{--N}(2\text{A})$

Table 1. Selected bond lengths [Å] and bond angles [°] for [Zn·1](NaClO₄) (values for two symmetry-independent molecules are given)

Zn(1)–O(1)	2.0839(14), 2.0665(4)	O(1)–Zn(1)–O(3)	94.70(6), 93.79(6)
Zn(1)–O(3)	2.1106(13), 2.1255(4)	O(1)–Zn(1)–N(1)	91.79(6), 93.10(6)
Zn(1)–N(1)	2.1555(17), 2.1766(17)	O(1)–Zn(1)–N(2)	83.21(6), 82.06(6)
Zn(1)–N(2)	2.1168(17), 2.1342(17)	O(1)–Zn(1)–N(3)	173.95(6), 174.18(6)
Zn(1)–N(3)	2.1600(17), 2.1477(17)	O(1)–Zn(1)–N(4)	97.88(6), 98.28(6)
Zn(1)–N(4)	2.1159(17), 2.1415(17)	O(3)–Zn(1)–N(1)	172.30(6), 170.20(6)
		O(3)–Zn(1)–N(2)	98.46(6), 102.32(6)
		O(3)–Zn(1)–N(3)	90.00(6), 89.91(6)
		O(3)–Zn(1)–N(4)	82.74(6), 81.57(6)
		N(1)–Zn(1)–N(2)	86.44(6), 85.52(6)
		N(1)–Zn(1)–N(3)	83.84(6), 83.80(6)
		N(1)–Zn(1)–N(4)	92.25(6), 90.55(6)
		N(2)–Zn(1)–N(3)	92.34(6), 92.76(6)
		N(2)–Zn(1)–N(4)	178.32(6), 176.07(6)
		N(3)–Zn(1)–N(4)	86.48(7), 86.70(7)

angle of 164.6(1)°. In accord with the higher charge of this cation, all Ga–N and Ga–O bonds are significantly shorter than the corresponding ones in the zinc(II) structure, with Ga(1)–N(1) at 2.046(2) Å, Ga(1)–N(2) at 2.078(2) Å, and especially Ga(1)–O(1) at 1.942(1) Å. Another noteworthy difference is the disparate carboxylate C–O distances here: 1.298(2) Å for the Ga-coordinated C(7)–O(1) versus 1.227(2) Å for the uncoordinated C(7)–O(2). In the zinc structure, these average to very similar values of 1.26 Å and 1.25 Å, respectively, most likely due to further coordination of the carbonyl oxygen atoms to sodium cations in the crystal lattice. Selected bond lengths and angles for this structure are listed in Table 2. The X-ray structure of a related gallium(III) complex of a DOTA derivative is in the published literature.^[13] A *cis*-N₄O₂ donor set is also found here with an axial N–Ga–N angle of 156.3°, Ga–N distances of 2.12–2.16 Å, and short Ga–O distances of 1.90–1.93 Å. Again, the coordinated carboxylate pendant arms are attached to the equatorial instead of axial cyclen nitrogen atoms. In the absence of the ethylene cross-bridge, the equatorial N–Ga–N angle opens up to 105.6°.

Figure 6. Molecular structure of [Ga-CB-DO2A]NO₃; hydrogen atoms and nitrate have been omitted for clarityTable 2. Selected bond lengths [Å] and bond angles [°] for [Ga·1]NO₃

Ga(1)–O(1)	1.9421(13)	O(1)–Ga(1)–O(1A)	90.28(8)
Ga(1)–N(1)	2.0461(15)	O(1)–Ga(1)–N(1)	165.20(5)
Ga(1)–N(2)	2.0780(15)	O(1)–Ga(1)–N(1A)	93.60(6)
		O(1)–Ga(1)–N(2)	83.23(6)
		O(1)–Ga(1)–N(2A)	107.90(6)
		N(1)–Ga(1)–N(1A)	86.24(9)
		N(1)–Ga(1)–N(2)	81.99(6)
		N(1)–Ga(1)–N(2A)	86.75(6)
		N(2)–Ga(1)–N(2A)	164.56(9)

Conclusion

Under basic conditions, Zn^{II}, Ga^{III}, and Cd^{II} complexes of the dicarboxylate pendant-armed cross-bridged cyclen H₂1 were prepared. In solution, both the Zn^{II} and Cd^{II} complexes were found by NMR spectroscopy to exhibit fast dynamic enantiomerization at room temperature; the Zn^{II} complex has a ΔG^\ddagger barrier of 12.3(1) kcal/mol at 24(2) °C. In contrast, the Ga^{III} complex exhibits C₂ symmetry consistent with its solid-state structure with no dynamic broadening on either the ¹H or ¹³C NMR timescales. X-ray structures confirm full ligand envelopment of both the Zn^{II} and Ga^{III} cations with significantly shorter Ga–N and Ga–O bonds. A dissociative enantiomerization mechanism is in agreement with the dramatically higher barrier of the Ga complex. These data, taken as a whole, infer that such pendant-armed ligand complexes of Ga^{III} will exhibit even greater kinetic stability than the parent cross-bridged complexes. Future kinetic inertness studies are clearly warranted.

Experimental Section

CAUTION: Although we did not encounter any problems, perchlorate salts of metal complexes containing organic ligands and solvents are potentially explosive and should be handled only in small quantities and with great caution!

General Methods and Materials: ^1H and $^{13}\text{C}\{^1\text{H}\}$ NMR spectra were recorded with a Bruker AM-360 or Varian Inova-400 instrument and referenced to TMS. Acetonitrile was used as an internal reference in D_2O with the methyl proton resonance set at $\delta = 2.06$ ppm and ^{13}C resonance at $\delta = 1.70$ ppm. Low-temperature ^1H and ^{13}C NMR spectral studies were carried out with the Varian Inova-400. A methanol chemical shift thermometer (0.03% concd. HCl in MeOH) was used to monitor the probe temperature.^[20] High-temperature spectra were recorded with the Bruker AM-360 and the probe temperature calculated from the chemical shift difference between the proton signals of neat ethylene glycol.^[21] Complete lineshape analysis of the two-site mutual exchange broadening exhibited by the $\delta = 61.77$ ppm room temperature $[24(2)^\circ\text{C}]$ $^{13}\text{C}\{^1\text{H}\}$ resonance of $[\text{Zn}\cdot\mathbf{1}]$ in CD_3OD (fast intermediate exchange) was carried out using the program WINDNMR-Pro version 7.1.5 (Hans J. Reich, University of Wisconsin, Madison, WI, USA, 2001),^[22] which is based on the modified Bloch equations as expressed by Rogers and Woodbrey;^[23] $\Delta\nu$ (484 Hz) was determined from the anisotropically broadened, slow-exchange limit spectrum (CD_3OD at -80°C). The simulations gave a rate constant k (forward = reverse) of $6.0(5) \times 10^3 \text{ s}^{-1}$. The ΔG^\ddagger at $24(2)^\circ\text{C}$ was calculated using the Eyring equation with $K = 1$. A lower limit was placed upon the enantiomerization barrier of $[\text{Ga}\cdot\mathbf{1}]^+$ in D_2O through comparison of the experimental proton ABX subspectrum of the pendant-arm CH_2 protons with simulated spectra (WINDNMR-Pro) allowing exchange of A and B nuclei. For $k = 1.5 \text{ s}^{-1}$, calculated broadening is significantly greater than that observed experimentally at $87(2)^\circ\text{C}$.

IR spectra were recorded as KBr pellets with a Nicolet MX-1 FT Spectrophotometer. Elemental analyses were obtained from Atlantic Microlab, Inc., Norcross, GA, USA. Reactions were run under nitrogen with magnetic stirring in standard Schlenk glassware. Bulk solvent removal was by rotary evaporation under reduced pressure and trace volatile removal from solids was by vacuum pump. Solvents were used as purchased. Cross-bridged ligand $\mathbf{1}$ ^[14,15] was pre-

pared as a trifluoroacetate salt by a modification of published methods.^[6]

$[\text{Zn}\cdot\mathbf{1}](\text{NaClO}_4)_{1.5}$: An aqueous solution of NaOH (0.970 N) (0.818 mL) was added to a MeOH solution (10 mL) of $\text{H}_2\mathbf{1}\cdot(\text{CF}_3\text{COOH})\cdot(\text{H}_2\text{O})$ (113 mg, 0.265 mmol) to form a clear solution. A MeOH solution (6 mL) of $\text{Zn}(\text{ClO}_4)_2\cdot 6\text{H}_2\text{O}$ (100 mg, 0.270 mmol) was then added into this solution. After refluxing for 2 d and cooling to room temperature, this MeOH solution was centrifuged off from a small amount of precipitate. Et_2O vapor diffusion into the supernatant yielded 106 mg (71.2%) of a white crystalline solid. IR (KBr): $\tilde{\nu} = 1617 \text{ cm}^{-1}$ (broad) (ν_{COO}). ^1H NMR (360.13 MHz, D_2O): $\delta = 3.63$ (s, 4 H, CH_2COO), 3.20–3.37 (m, 8 H), 3.03 (s, 4 H, cross-bridging CH_2CH_2), 2.89–3.08 (m, 8 H) ppm. ^1H NMR (400 MHz, CD_3OD): $\delta = 3.61$ (s, 4 H, CH_2COO), 3.20–3.41 (m, 8 H), 3.07 (s, 4 H, cross-bridging CH_2CH_2), 2.91–3.15 (m, 8 H) ppm. ^1H NMR (400 MHz, CD_3OD , -80°C): $\delta = 3.72$ (AB, CH_2COO , $J = 16.4 \text{ Hz}$, 4 H), 3.24–3.48 (m, 8 H), 2.72–3.19 (m, 12 H) ppm. $^{13}\text{C}\{^1\text{H}\}$ (D_2O): $\delta = 179.03$, 64.94, 61.10, 56.83, 49.95 ppm. $^{13}\text{C}\{^1\text{H}\}$ NMR (100 MHz, CD_3OD): $\delta = 177.85$, 66.11, 61.77 (br.), 57.85, 50.80 ppm. $^{13}\text{C}\{^1\text{H}\}$ NMR (100 MHz, CD_3OD , -80°C): $\delta = 178.59$, 65.62, 63.93, 59.12, 58.44, 56.89, 50.12 ppm. $\text{C}_{14}\text{H}_{24}\text{Cl}_{1.5}\text{N}_4\text{Na}_{1.5}\text{O}_{10}\text{Zn}$ (561.41): calcd. C 29.95, H 4.31, N 9.98; found C 30.05, H 4.68, N 9.81. X-ray quality crystals were grown by ether diffusion into a sample dissolved in 95% ethanol solution. These have a composition of $[\text{Zn}\cdot\mathbf{1}](\text{NaClO}_4)(\text{C}_2\text{H}_5\text{OH})(\text{H}_2\text{O})_{0.5}$.

$[\text{Cd}\cdot\mathbf{1}](\text{NaClO}_4)(\text{H}_2\text{O})_{1.5}$: An aqueous solution of NaOH (0.970 N) (0.64 mL) was added to a clear solution of $\text{H}_2\mathbf{1}\cdot(\text{CF}_3\text{COOH})\cdot(\text{H}_2\text{O})$ (89.0 mg, 0.208 mmol) and $\text{Cd}(\text{ClO}_4)_2\cdot 6\text{H}_2\text{O}$ (94.8 mg, 0.226 mmol) in 15 mL MeOH to form a cloudy solution. The reaction mixture was refluxed for 7 h, cooled, and some white precipitate was centrifuged off. Et_2O vapor diffusion into the supernatant yielded 73.0 mg (61.1%) of a white crystalline solid. IR (KBr): $\tilde{\nu} = 1615$, 1595 cm^{-1} (ν_{COO}). ^1H NMR (360.13 MHz, D_2O):

Table 3. Crystallographic data for $[\text{Zn}\cdot\mathbf{1}](\text{NaClO}_4)$ and $[\text{Ga}\cdot\mathbf{1}]\text{NO}_3$

	$[\text{Zn}\cdot\mathbf{1}](\text{NaClO}_4)$	$[\text{Ga}\cdot\mathbf{1}]\text{NO}_3$
Empirical formula	$\text{C}_{16}\text{H}_{31}\text{ClN}_4\text{NaO}_{9.50}\text{Zn}$	$\text{C}_{14}\text{H}_{24}\text{GaN}_5\text{O}_7$
Formula mass	555.26	444.10
Crystal system, space group	monoclinic, $P2_1/c$	orthorhombic, $P2_12_12$
a [Å]	16.2288(10)	8.7107(7)
b [Å]	9.3084(6)	12.5119(10)
c [Å]	29.0705(18)	7.5586(6)
α [°]	90.0	90.0
β [°]	95.564(1)	90.0
γ [°]	90.0	90.0
V [Å ³]	4370.8(5)	823.79(11)
Z	8	2
T [K]	150(2)	218(2)
λ [Å]	0.71073 (Mo- K_α)	0.71073 (Mo- K_α)
$\rho_{\text{calcd.}}$ [g·cm ⁻³]	1.688	1.790
μ [mm ⁻¹]	1.326	1.724
Measured reflections	27282	6004
Independent reflections	10255 ($R_{\text{int}} = 0.028$)	1967 ($R_{\text{int}} = 0.0260$)
Independent reflections	9175	1872
$R^{\text{[a]}}$, $R^{\text{[b]}}(\omega F^2)$ (obsd. data)	0.0347; 0.0853	0.0231; 0.0553
$R^{\text{[a]}}$, $R^{\text{[b]}}(\omega F^2)$ (all data)	0.0412; 0.0853	0.0244; 0.0557
GOF	1.143	1.006

^[a] $R = \Sigma ||F_o| - |F_c|| / \Sigma |F_o|$. ^[b] $R(\omega F^2) = \{\Sigma [\omega(F_o^2 - F_c^2)^2] / \Sigma [\omega(F_o^2)^2]\}^{1/2}$; $\omega = 1/[\sigma^2(F_o^2) + (aP)^2 + bP]$, $P = [2F_c^2 + \max(F_o, 0)]/3$.

$\delta = 3.48$ (s, 4 H, CH_2COO , ^{111}Cd , ^{113}Cd satellites, $J = 11.6$ Hz), 2.94–3.26 (m, 12 H), 2.89 (s, 4 H, cross-bridging CH_2CH_2 , ^{111}Cd , ^{113}Cd satellites, $J = 13.7$ Hz), 2.81 (br. dd, 4 H, $J = 12.1$, 4.4 Hz) ppm. $^{13}\text{C}\{^1\text{H}\}$ NMR (90.55 MHz, D_2O): $\delta = 179.23$ (^{111}Cd , ^{113}Cd satellites, $J = 11.3$ Hz), 64.95 (^{111}Cd , ^{113}Cd satellites, $J = 6.0$ Hz), 60.58, 57.32, 47.63 (^{111}Cd , ^{113}Cd satellites, $J = 15.3$ Hz) ppm. $\text{C}_{14}\text{H}_{27}\text{CdClN}_4\text{NaO}_{9.5}$ (574.24): calcd. C 29.28, H 4.74, N 9.76, Cl 6.17; found C 29.31, H 4.70, N 9.65, Cl 5.96.

[Ga·1](NO₃)₃: A solution of $\text{Ga}(\text{NO}_3)_3$ hydrate (38.6 mg, ca. 0.15 mmol) in MeOH (6 mL) was added to an MeOH solution (14 mL) of $\text{H}_2\text{I}(\text{CF}_3\text{COOH})\cdot(\text{H}_2\text{O})$ (66.4 mg, 0.155 mmol) to form a clear solution. Anhydrous NaOAc (46.3 mg, 0.564 mmol) in MeOH (7 mL) was then added in two portions. The reaction mixture was refluxed for 2 d, after which time a white precipitate was isolated by centrifugation. The resulting white precipitate was dried to give the product complex (41.9 mg, 62.9%). This was redissolved in a H_2O (2.6 mL)/MeOH (3.2 mL) mixture followed by Et_2O /MeOH (1:1) vapor diffusion into this solution to yield crystals suitable for X-ray analyses. IR (KBr): $\tilde{\nu} = 1692$ (s), 1672 (s) cm^{-1} (ν_{COO}), 1363 (s), 1351 (s), 1339 (s), 1299 (s), 1284 (s) cm^{-1} (broad) (ν_{NO_3}). ^1H NMR (360.13 MHz, D_2O): $\delta = 4.03$ and 4.06 (AB of apparent ABX , CH_2COO , $J_{AB} = 16.8$, $J_{BX} \approx 1.5$ Hz, 4 H), 3.57–3.85 (m, 10 H), 3.38–3.54 (m, 6 H), 3.18–3.31 (m, 4 H, cross-bridging CH_2CH_2) ppm. $^{13}\text{C}\{^1\text{H}\}$ NMR (90.55 MHz, D_2O): $\delta = 174.89$, 64.07, 63.67, 57.11, 57.09, 54.87, 51.78 ppm. $^{13}\text{C}\{^1\text{H}\}$ NMR (90.55 MHz, $[\text{D}_6]\text{DMSO}$): $\delta = 169.92$, 63.65, 61.92, 56.21, 55.35, 54.06, 50.25 ppm. $\text{C}_{14}\text{H}_{24}\text{Ga}_2\text{N}_5\text{O}_7$ (444.10): calcd. C 37.86, H 5.45, N 15.77; found C 37.82, H 5.45, N 15.75.

X-ray Crystallography: Diffraction intensity data were collected with Bruker Smart Apex CCD $\{[\text{Zn}\cdot 1](\text{NaClO}_4)\}$ and Siemens P4 CCD $\{[\text{Ga}\cdot 1]\text{NO}_3\}$ diffractometers. Crystal data collection, and refinement parameters are given in Table 3. The structures were solved using direct methods, completed by subsequent difference Fourier syntheses, and refined by full-matrix least-squares procedures on F^2 . SADABS absorption corrections were applied to both sets of data ($T_{\text{min}}/T_{\text{max}} = 0.917$ and 0.724 for $[\text{Zn}\cdot 1](\text{NaClO}_4)$ and $[\text{Ga}\cdot 1]\text{NO}_3$, respectively). In both structures all non-hydrogen atoms were refined with anisotropic displacement coefficients. Hydrogen atoms were treated as idealized contributions except the H atoms of solvent water molecules in $[\text{Zn}\cdot 1](\text{NaClO}_4)$ involved in H-bonds which were located on the F-map and refined with isotropic thermal parameters. The Flack parameter for $[\text{Ga}\cdot 1]\text{NO}_3$ is 0.014(11). All software and sources of scattering factors are contained in the SHELXTL (5.10) program package (G. Sheldrick, Bruker XRD, Madison, WI, USA). CCDC-229393 $\{[\text{Zn}\cdot 1](\text{NaClO}_4)\}$ and -229394 $\{[\text{Ga}\cdot 1]\text{NO}_3\}$ contain the supplementary crystallographic data for this paper. These data can be obtained free of charge at www.ccdc.cam.ac.uk/conts/retrieving.html [or from the Cambridge Crystallographic Data Centre, 12 Union Road, Cambridge CB2 1EZ, UK; Fax: (internat.) + 44-1223-336-0333; E-mail: deposit@ccdc.cam.ac.uk].

Acknowledgments

Financial support of this research was from NIH grants CA93375 and GM55916-01 at UNH and an NSF instrumentation grant at the University of California, San Diego.

- [1] X. Sun, M. Wuest, G. R. Weisman, E. H. Wong, D. P. Reed, R. J. Motekaitis, A. E. Martell, M. J. Welch, C. J. Anderson, *J. Med. Chem.* **2002**, 45, 469–477.
- [2] C. A. Boswell, X. Sun, W. Niu, G. R. Weisman, E. H. Wong, A. L. Rheingold, C. J. Anderson, *J. Med. Chem.* **2004**, 47, 1465–1474.
- [3] J. Springborg, *Dalton Trans.* **2003**, 1653–1665.
- [4] T. J. Hubin, *Coord. Chem. Rev.* **2003**, 241, 27–46.
- [5] G. R. Weisman, M. E. Rogers, E. H. Wong, J. P. Jasinski, E. S. Paight, *J. Am. Chem. Soc.* **1990**, 112, 8604–8605.
- [6] G. R. Weisman, E. H. Wong, D. C. Hill, M. E. Rogers, D. P. Reed, J. C. Calabrese, *Chem. Commun.* **1996**, 947–948.
- [7] E. H. Wong, G. R. Weisman, D. C. Hill, D. P. Reed, M. E. Rogers, J. P. Condon, M. A. Fagan, J. C. Calabrese, K.-C. Lam, I. A. Guzei, A. L. Rheingold, *J. Am. Chem. Soc.* **2000**, 122, 10561–10572.
- [8] J. Chin, M. Banaszczyk, V. Jubian, X. Zou, *J. Am. Chem. Soc.* **1989**, 111, 186–90.
- [9] R. Hettich, H.-J. Schneider, *J. Am. Chem. Soc.* **1997**, 119, 5638–5647.
- [10] J. A. Halfen, S. Mahapatra, E. C. Wilkinson, S. Kaderli, V. G. Young Jr., L. Que Jr., A. D. Zuberbuehler, W. B. Tolman, *Science (Washington, D. C.)* **1996**, 271, 1397–1400.
- [11] C. J. Anderson, M. J. Welch, *Chem. Rev.* **1999**, 99, 2219–2234.
- [12] D. E. Reichert, J. S. Lewis, C. J. Anderson, *Coord. Chem. Rev.* **1999**, 184, 3–66.
- [13] A. Heppeler, S. Froidevaux, H. R. Macke, E. Jermann, M. Behe, P. Powell, M. Hennig, *Chem. Eur. J.* **1999**, 5, 1974–1981.
- [14] D. A. Moore (Mallinckrodt Medical, Inc., USA), in *PCT Int. Appl. Wo*, **1994**, pp. 58ff.
- [15] H. S. Winchell, J. Y. Klein, E. D. Simhon, R. L. Cyjon, O. Klein, H. Zaklad (Concat, Inc., USA), in *U.S.*, **1999**, pp. 41ff, Cont.-in-part of U.S. Ser. No. 560,626.
- [16] W. Niu, E. H. Wong, G. R. Weisman, L. N. Zakharov, C. D. Incarvito, A. L. Rheingold, *Polyhedron* **2004**, 23, 1019–1025.
- [17] W. Niu, E. H. Wong, G. R. Weisman, D. C. Hill, K.-C. Lam, R. D. Sommer, L. N. Zakharov, A. L. Rheingold, manuscript in preparation.
- [18] T. J. Hubin, N. W. Alcock, M. D. Morton, D. H. Busch, *Inorg. Chim. Acta* **2003**, 348, 33–40.
- [19] A. Riesen, M. Zehnder, T. A. Kaden, *Acta Crystallogr., Sect. C: Cryst. Struct. Commun.* **1991**, 47, 531–533.
- [20] A. L. Van Geet, *Anal. Chem.* **1970**, 42, 679–680.
- [21] M. L. Kaplan, F. A. Bovey, H. N. Cheng, *Anal. Chem.* **1975**, 47, 1703.
- [22] H. J. Reich, *J. Chem. Educ.: Software, Ser. D* **1996**, 3, 17–19, 27–33, 56–66.
- [23] J. Sandström, in *Dynamic NMR Spectroscopy*, Academic Press, New York, **1982**, p. 14.

Received January 29, 2004
Early View Article
Published Online June 11, 2004